ELSEVIER

Available online at www.sciencedirect.com

ScienceDirect

International Journal of Solids and Structures 43 (2006) 6329–6346

INTERNATIONAL JOURNAL OF SOLIDS and STRUCTURES

www.elsevier.com/locate/ijsolstr

Approximation of the flexural velocity branch in plates

O. Poncelet [a,*], A.L. Shuvalov [a], J. Kaplunov [b,1]

[a] *Laboratoire de Mécanique Physique, Université Bordeaux 1, UMR CNRS 5469, 351, Cours de la Libération, F-33405 Talence Cedex, France*

[b] *Department of Mathematics, University of Manchester, Oxford Road, Manchester M13 9PL, UK*

Received 4 June 2005; received in revised form 14 June 2005
Available online 7 October 2005

Abstract

The fitting of the flexural velocity branch by means of the Padé approximation is examined. Its use for free isotropic plates is elaborated and compared to other approaches. The flexural-velocity expansion into power series, which underlies the Padé implementation, is detailed. The generalization for fluid-loaded plates and inhomogeneous plates is outlined, and the impact of anisotropy is discussed in some detail.

Keywords: Elastic plate; Flexural branch; Padé approximation

1. Introduction

Approximation of the flexural mode in an isotropic plate lies at the heart of many theoretical and practical applications. The starting point is usually the classical Kirchhoff thin-plate theory, providing the leading-order evaluation for long waves. It admits various well-known lines of development described in the extensive literature (e.g., Graff, 1991; Kaplunov et al., 1998; Le, 1999). In particular the higher-order asymptotic plate theories improve approximation of the flexural branch over the long-wave domain, however, they are generally not applicable for the short-wave/high-frequency range (see a detailed discussion by Goldenveizer et al., 1993; Kaplunov et al., 1998). At the same time, there is often a need for explicit estimation of the full range of the flexural velocity branch, otherwise defined exactly but implicitly by a transcendental equation. This purpose is pursued by the engineering shear-deformation plate theories,

* Corresponding author. Tel.: +33 5 40 00 21 91; fax: +33 5 40 00 69 64.
E-mail address: o.poncelet@lmp.u-bordeaux1.fr (O. Poncelet).
[1] Present address: Department of Mathematical Sciences, Brunel University, Uxbridge, Middlesex UB8 3PH, UK.

0020-7683/$ - see front matter
doi:10.1016/j.ijsolstr.2005.07.031

which involve certain adjustable parameters and ad hoc assumptions for extending the velocity approximation whilst leaving wave-field modelling at the background (for more details, see the review by Altenbach, 2000). The benchmark for such approaches is Mindlin's (1951) theory using either the shear correction only, or complementing it by the account of rotary inertia. Correspondingly, the flexural velocity branch in a traction-free isotropic plate with the density ρ, Young's modulus E, and Poisson's ratio ν is approximated by the following formulas (Mindlin, 1951):

$$v_{\mathrm{f}}(k) \approx \frac{\kappa k d}{\sqrt{1+(\kappa k d)^2/c_{\mathrm{R}}^2}},$$
$$v_{\mathrm{f}}(k) \approx \sqrt{6}\left[\kappa^2 + c_{\mathrm{R}}^2\left(\frac{1}{12}+\frac{1}{(kd)^2}\right) - \sqrt{\left(\kappa^2 + c_{\mathrm{R}}^2\left(\frac{1}{12}+\frac{1}{(kd)^2}\right)\right)^2 - \frac{c_{\mathrm{R}}^2\kappa^2}{3}}\right]^{1/2}, \tag{1}$$

where $k=\omega/v$ is the horizontal wave number; d is the plate thickness;

$$\kappa = \frac{c_{\mathrm{b}}}{\sqrt{12(1-\nu^2)}} \tag{2}$$

is the Kirchhoff's dispersion coefficient[2] describing the slope of the exact flexural branch $v_{\mathrm{f}}(k)$ at the origin point $k=0$; $c_{\mathrm{b}}=\sqrt{E/\rho}$ is the bar velocity; and c_{R} is the Rayleigh surface-wave velocity, imposed as the short wave limit by the shear correction. Among these two approximations—without and with rotary inertia—the latter yields a notably better fit for relatively long waves but the former is more accurate for short waves. From a numerical viewpoint, a remarkable efficiency of the simple formula $(1)_1$ is fostered by the advantageous competition of the long- and short-wave trends: with growing kd, the curve $(1)_1$ first lies slightly above the exact branch $v_{\mathrm{f}}(k)$, then crosses $v_{\mathrm{f}}(k)$ and tends to c_{R} from below. Eqs. (1) may be re-written in terms of frequency dependence, correspondingly, as

$$v_{\mathrm{f}}(\omega) \approx \sqrt{\kappa\omega d}\left(\sqrt{\frac{(\kappa\omega d)^2}{4c_{\mathrm{R}}^4}+1} - \frac{\kappa\omega d}{2c_{\mathrm{R}}^2}\right)^{1/2},$$
$$v_{\mathrm{f}}(\omega) \approx \sqrt{\frac{6}{1-12c_{\mathrm{R}}^2/\omega d}}\left[\left(\kappa^2+\frac{c_{\mathrm{R}}^2}{12}\right) - \sqrt{\left(\kappa^2-\frac{c_{\mathrm{R}}^2}{12}\right)^2 + \frac{c_{\mathrm{R}}^2\kappa^2}{3}}\right]^{1/2}. \tag{3}$$

Note in passing that Eq. $(3)_1$, inferred from $(1)_1$, is a better approximant than the estimate $v_{\mathrm{f}}^2(\omega)\approx \kappa\omega d/(1+\kappa\omega d/c_{\mathrm{R}}^2)$, formally constructed on the same grounds as $(1)_1$ but lacking the advantageous counterbalance of the long and short wave trends. Concerning the evaluation of c_{R} involved in these and other approximations to be discussed, one may consult the review by Destrade (2003) with ample bibliography and also Achenbach (1973), Pham Chi Vinh and Ogden (2004a,b).

Improvements to Mindlin's approximation have been sought via other model assumptions that avoid the shear correction (Jemielita, 1990; Muller and Touratier, 1995; Altenbach, 2000), or via optimizing its value for the best numerical fit of the flexural velocity branch (see Goldenveizer et al., 1990 and the references there; also Goldenveizer et al., 1993; Stephen, 1997; Kaplunov et al., 1998). In the latter literature it has been found that the shear correction, which instead of imposing the Rayleigh limit verifies the correct

[2] Throughout the paper, κ stands for the slope of the flexural branch in isotropic and then in anisotropic and inhomogeneous plates, as has been adopted in the previous authors' publications, though this notation may appear awkward in the present context because of the conventional use of κ for denoting the shear coefficient.

second-order Taylor coefficient of, specifically, the refined (with rotary inertia) Mindlin theory prediction, modifies $(1)_2$ by means of replacement

$$c_{\mathrm{R}}^2 \to c_{\mathrm{t}}^2 \frac{5}{6-\nu}, \tag{4}$$

where c_{t} is the transverse-wave velocity. Such replacement improves, as desired, the long-wave fit, while still keeping the short wave limit fairly close to c_{R}. The estimate using $(1)_2$ with (4) will be referred henceforth as the optimized Mindlin's approximation.

The objective of this paper is, firstly, to elucidate the derivation of coefficients of the exact power-series expansion of flexural velocity and, secondly, to explore on this basis the capacity of the Padé approximation for evaluating the flexural velocity branch in full. The expediency is noted for modifying the Padé scheme by enforcing the Rayleigh limit, whereby the first order of this approximation is Mindlin's formula $(1)_1$. The main part of the paper (Sections 2 and 3; Appendices A and B) is concerned with free isotropic plates. The potential of applying the same recipes to fitting the flexural velocity branch in a broader context involving immersed, anisotropic and inhomogeneous plates is pointed out in Section 4 (see also Appendix C). The results of this study are hoped to be useful for various applications involving numerical or analytical evaluation of the flexural velocity dispersion. From the prospective viewpoint, the Padé approximation of the flexural-branch dispersion stimulates development of a mathematically consistent plate theory with correct long-wave and short-wave limits. A short-wave prerequisite is the recent derivation of the low-dimensional explicit asymptotic models for surface waves (Kaplunov and Kossovich, 2004; Kaplunov et al., 2004).

2. Power series and short wave asymptotics

An exact solution for the free-plate flexural velocity, defined by a transcendental equation in v^2 and kd, is certainly out of reach. At the same time, its Taylor series can be recovered, in principle, up to any order by way of expanding the dispersion relation in powers of kd and tracing the Taylor coefficients for flexural-velocity solution recursively (note the difference with the asymptotic-method solving the truncated polynomial equation). The squared velocity $v_{\mathrm{f}}^2(k)$ expands in even powers: $v_{\mathrm{f}}^2(k) = \sum_{n=1}^{\infty} A_{2n}(kd)^{2n}$, where the leading order coefficient is $A_2 = \kappa^2$. For the case of isotropic plates, the structure of coefficients of this series and of the related ones can be specified so that

$$\begin{aligned} v_{\mathrm{f}}^2(k) &= \kappa^2 \sum_{n=1}^{\infty} \frac{a_{2n}}{(2n+1)!(1-\nu)^{n-1}}(kd)^{2n}, \qquad v_{\mathrm{f}}(k) = \kappa \sum_{n=1}^{\infty} \frac{b_{2n-1}}{(3n-1)!(1-\nu)^{n-1}}(kd)^{2n-1}, \\ v_{\mathrm{f}}^2(\omega) &= \kappa^2 \sum_{n=1}^{\infty} \frac{c_n}{(3n-1)!(1-\nu)^{n-1}}\left(\frac{\omega d}{\kappa}\right)^{n-1}, \qquad v_{\mathrm{f}}(\omega) = \kappa\sqrt{\frac{\omega d}{\kappa}} \sum_{n=1}^{\infty} \frac{d_n}{(3n)!(1-\nu)^{n-1}}\left(\frac{\omega d}{\kappa}\right)^{n-1}. \end{aligned} \tag{5}$$

The first four coefficients in the series (5) are as follows:

$$\begin{aligned} &a_2 = 6, \quad a_4 = 2(7\nu - 17), \quad a_6 = 62\nu^2 - 418\nu + 489, \\ &a_8 = \frac{6}{5}(381\nu^3 - 4995\nu^2 + 14,613\nu - 11,189); \\ &b_1 = 2, \quad b_3 = 7\nu - 17, \quad b_5 = \frac{1}{5}(897\nu^2 - 6694\nu + 7757), \\ &b_7 = \frac{33}{20}(8961\nu^3 - 137,693\nu^2 + 416,423\nu - 315,691); \end{aligned}$$

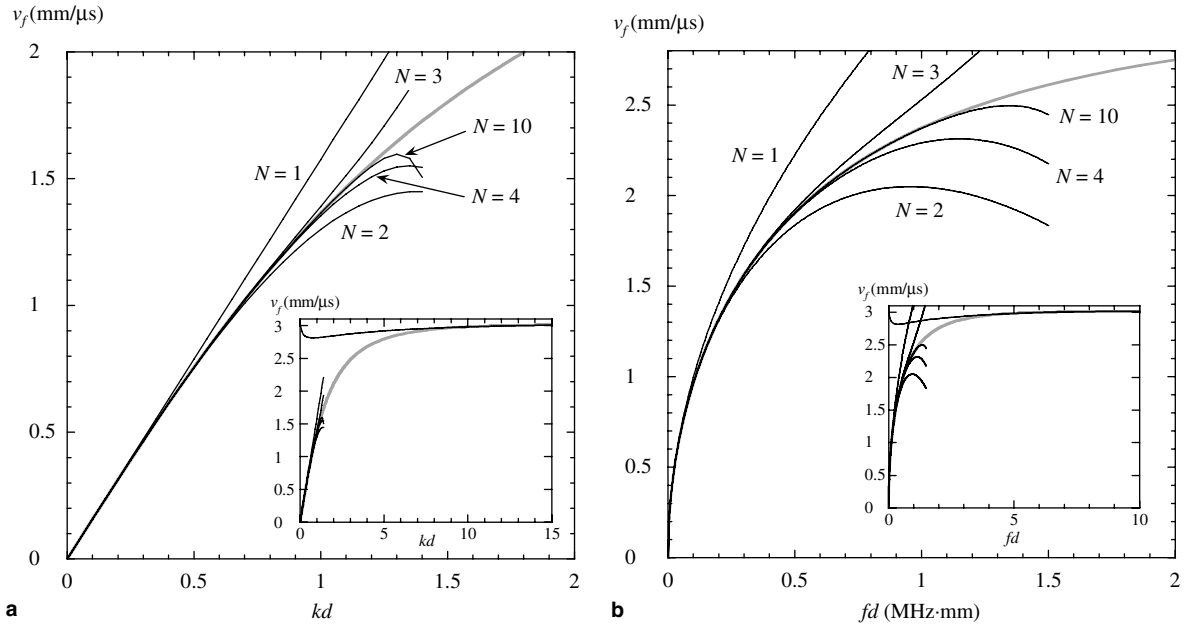

Fig. 1. Long wave power-series approximation by the truncated power series (5) and (6) for the flexural branch $v_f(k)$ (a) and $v_f(\omega)$ (b) in a steel plate. Thick gray line is the exact curve, thin black curves are the approximations by the power series with N terms retained. The insets show the short wave asymptotics (7).

$$
\begin{aligned}
&c_1 = 2, \quad c_2 = 7v - 17, \quad c_3 = \frac{1}{5}(211v^2 - 3362v + 3711),\\
&c_4 = -\frac{132}{5}(17v^3 + 1334v^2 - 5129v + 3603);\\
&d_1 = 6, \quad d_2 = 3(7v - 17), \quad d_3 = \frac{9}{20}(79v^2 - 5058v + 5399),\\
&d_4 = -\frac{99}{40}(1641v^3 + 48,627v^2 - 204,477v + 138,809)
\end{aligned}
\tag{6}
$$

(an adaption of these coefficients for the series $k_f^4(\omega^2)$ is given in Goldenveizer et al., 1993; Kaplunov et al., 1998). A few more coefficients a_{2n} are listed in the Appendix A.

The efficiency of approximating the flexural velocity by the truncated power series is restricted to within the range of long waves. Further extending the fitting domain requires progressively increasing number of terms of the power series and soon becomes impractical. This is exemplified by Fig. 1 for a steel plate.[3] At the same time, the value of the Taylor expansion goes beyond its usage for direct fitting, as the coefficients of this series are engaged in constructing Padé approximants, see Section 3.

Taking the inverse perspective, consider the short wave asymptotics

$$
\frac{v_R - v_f(k)}{v_R} \approx \frac{e^{-q_t kd} - e^{-q_l kd}}{\eta_R^2\left[\dfrac{\eta_R^4(2v-1) + \eta_R^2(2.5-2v) - 1}{8(q_l q_t)^{5/2}(1-v)} + \dfrac{2}{q_t} kd e^{-q_t kd}\right]},
\tag{7}
$$

[3] The material parameters of steel used in the calculations are: $\rho = 7.932$ g/cm^3, longitudinal and transverse velocity $c_l = 5.96$ and $c_t = 3.26$ mm/μs, yielding $E = 216.9$ GPa, $v = 0.29$.

where $\eta_R = c_R/c_t$ and $q_{l,t} = \sqrt{1 - c_R^2/c_{l,t}^2}$. With kd decreasing from infinity, Eq. (7) follows the flexural branch only until its notable departure from the Rayleigh plateau and usually does not match with the power-series approximation (see inset to Fig. 1).

3. Padé approximation

Given a function $f(x)$, defined by a power series in x up to the $(N+M)$th power, its Padé approximation $f_{N,M}(x)$ for each pair N, M adding up to a given sum $N+M$ is a fractional rational function, which is a ratio of polynomials Nth and Mth degree. Their coefficients are identified by the first $N+M$ coefficients of the series for $f(x)$ about $x=0$ through the condition that $f(x)$ is approximated by $f_{N,M}(x)$ up to the order of $N+M$ (Baker and Graves-Morris, 1996).

It is clear by definition that, once the Taylor coefficients are known, the Padé approximation can provide any desirable accuracy of the long-wave fit and, moreover, extend the fitting range comparatively to the underlying Taylor series. What is more interesting is trying this approximation for the whole branch. The flexural velocity v_f with growing k or ω tends to a constant, so the Padé approximant of its full extent is to be sought as a ratio of polynomials of the same degree. Therefore, in view of (5), it is specifically the squared velocity that must be invoked. Consider $v_f^2(k)$, whose Taylor expansion $(5)_1$ is in even powers of k and hence so are the polynomials of its Padé approximants. Knowing an *even* number N of the coefficients $a_2,\dots,a_{2N}$ in $(5)_1$ allows us to introduce the Padé approximant $\left[v_f^2(k)\right]_{N,N}$:

$$\left[v_f^2(k)\right]_{N,N} = \kappa^2 \frac{\alpha_2^{(N,N)}(kd)^2 + \cdots + \alpha_N^{(N,N)}(kd)^N}{\alpha_2^{(N,N)} + \beta_2^{(N,N)}(kd)^2 + \cdots + \beta_N^{(N,N)}(kd)^N} \quad (N \text{ is even}), \tag{8}$$

which, by construction, ensures the dispersion equation validity up to the order $2N$ in k and tends at $kd \to \infty$ to a constant. For example, by appeal to $a_2,\dots,a_8$ given in (6), the coefficients for the first two Padé approximants (8),

$$\left[v_f^2(k)\right]_{2,2} = \kappa^2 \frac{\alpha_2^{(2,2)}(kd)^2}{\alpha_2^{(2,2)} + \beta_2^{(2,2)}(kd)^2}, \qquad \left[v_f^2(k)\right]_{4,4} = \kappa^2 \frac{\alpha_2^{(4,4)}(kd)^2 + \alpha_4^{(4,4)}(kd)^4}{\alpha_2^{(4,4)} + \beta_2^{(4,4)}(kd)^2 + \beta_4^{(4,4)}(kd)^4} \tag{9}$$

are as follows:

$$\begin{aligned}
\alpha_2^{(2,2)} &= 60(1-\nu), \quad \beta_2^{(2,2)} = 17 - 7\nu,\\
\alpha_2^{(4,4)} &= 5040(1-\nu)^2(33\nu^2 + 424\nu - 422),\\
\alpha_4^{(4,4)} &= -168(1-\nu)(17\nu^3 + 1334\nu^2 - 5129\nu + 3603),\\
\beta_2^{(4,4)} &= -420(1-\nu)(53\nu^3 + 1015\nu^2 - 4084\nu + 2876),\\
\beta_4^{(4,4)} &= 551\nu^4 + 30,934\nu^3 - 133,642\nu^2 + 243,188\nu - 135,886
\end{aligned} \tag{10}$$

(see also Appendix B). Note that the short-wave limit $\kappa^2\alpha_N^{(N,N)}/\beta_N^{(N,N)}$ of the Padé approximants $\left[v_f^2\right]_{N,N}$ does not offer a uniform tendency to c_R^2 with growing N. Moreover, its value $10c_t^2/(17-7\nu)$ for $N=2$ is much farther from c_R^2 than the limit $5c_t^2/(6-\nu)$ of optimized Mindlin's approximation (see (4)), which is also stipulated by plugging the 'true' second-order Taylor coefficient but is not of the Padé rational form $(9)_1$.

The Padé scheme can be altered by enforcing the correct (Rayleigh) short-wave limit, so that the 'modified' Padé approximant

$$\left[\widetilde{v}_f^2(k)\right]_{N,N} = \kappa^2 \frac{\widetilde{\alpha}_2^{(N,N)}(kd)^2 + \cdots + \widetilde{\alpha}_N^{(N,N)}(kd)^N}{\widetilde{\alpha}_2^{(N,N)} + \widetilde{\beta}_2^{(N,N)}(kd)^2 + \cdots + \left(\kappa^2\widetilde{\alpha}_N^{(N,N)}/c_R^2\right)(kd)^N} \quad (N \text{ is even}) \tag{11}$$

is stipulated by equality of its Taylor series in k^2 to that of exact $v_f^2(k)$ up to the order $N-1$ in k^2, whereas, in distinction to (8), conditioning equality of the Nth order Taylor coefficient of $[\widetilde{v}_f^2]_{N,N}$ to that of v_f^2 is replaced by imposing the short-wave limit c_R^2 (hence $\widetilde{\alpha},\widetilde{\beta}\neq\alpha,\beta$). This definition leads to a system of *linear* equations, which enables us to express the sought-for N coefficients of $[\widetilde{v}_f^2(k)]_{N,N}$ via c_R^2 and the coefficients $a_2,\ldots,a_{2N-2}$ of $(5)_1$. The first modified Padé approximant $[\widetilde{v}_f^2]_{2,2}$ is indeed nothing other than the (squared) Mindlin's approximation with shear correction $(1)_1$. The coefficients of the second modified Padé approximant $[\widetilde{v}_f^2]_{4,4}$ are

$$\widetilde{\alpha}_2^{(4,4)}=12(1-\nu)\left[\frac{5}{1+\nu}(c_b^2/c_R^2)-17+7\nu\right],\qquad \widetilde{\alpha}_4^{(4,4)}=\frac{1}{140}(132\nu^2+1696\nu-1688),$$
$$\widetilde{\beta}_2^{(4,4)}=-\frac{1}{7}(62\nu^2-418\nu+489)+\frac{17-7\nu}{1+\nu}(c_b^2/c_R^2). \tag{12}$$

Application of the Padé approximation for the flexural branch in a steel plate is demonstrated in Fig. 2 in comparison with Mindlin's formulas (1) and the optimized version with (4). In order to examine the accuracy of approximations for various isotropic materials, it is noted that the ratio of $v_f(k)$ to $c_b=\sqrt{E/\rho}$ depends only on the Poisson's ratio ν and kd, hence the shapes of the flexural branch $v_f(kd)$ in isotropic plates are represented, to within a uniform scaling factor $\sqrt{E/\rho}$, by the surface $\phi(\nu,kd)=v_f(k)/c_b$. The relative discrepancy of evaluating several cuts $kd=$ const. of this surface by different approximations is shown in Fig. 3 as a function of ν.

On inspecting Figs. 2 and 3, it is seen that raising the order N of the Padé approximations $v_f(k)\approx\sqrt{[v_f^2(k)]_{N,N}}$ (the curves N,N), which by definition increases the fitting precision in the long- and medium-wave range, actually decreases the short-wave accuracy once $N>6$. Also by definition, the use of the modified Padé approximation with the enforced Rayleigh limit (including Mindlin's fit $(1)_1$, labeled

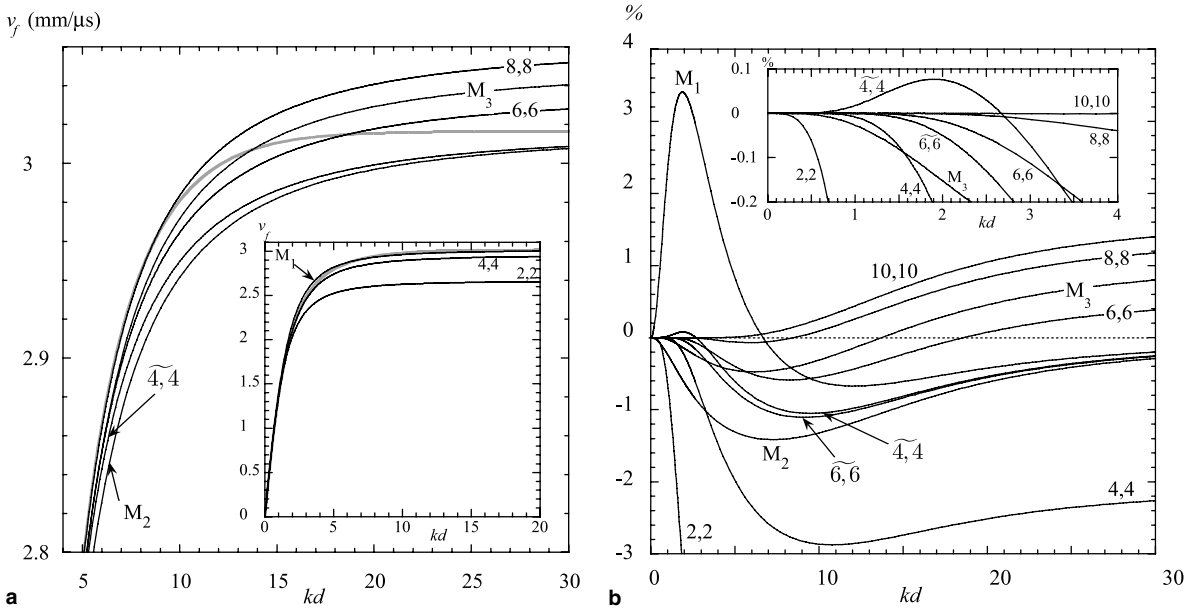

Fig. 2. Different approximations of the flexural branch $v_f(k)$ in a steel plate. (a) Thick gray line is the exact curve. Thin black lines are the fittings: by Mindlin's formulas $(1)_{1,2}$ (labeled M_1 and M_2); by $(1)_2$ optimized via (4) (labeled M_3); by the (square roots of) the Padé approximants $[v_f^2(k)]_{N,N}$ (labeled N,N) and the modified Padé approximant $[\widetilde{v}_f^2(k)]_{N,N}$ (labeled $\widetilde{N,N}$), see (8)–(12). (b) Relative discrepancy of the approximations $\left(v_f^{(\text{approx})}-v_f^{(\text{exact})}\right)/v_f^{(\text{exact})}$ in % (labels mean the same).

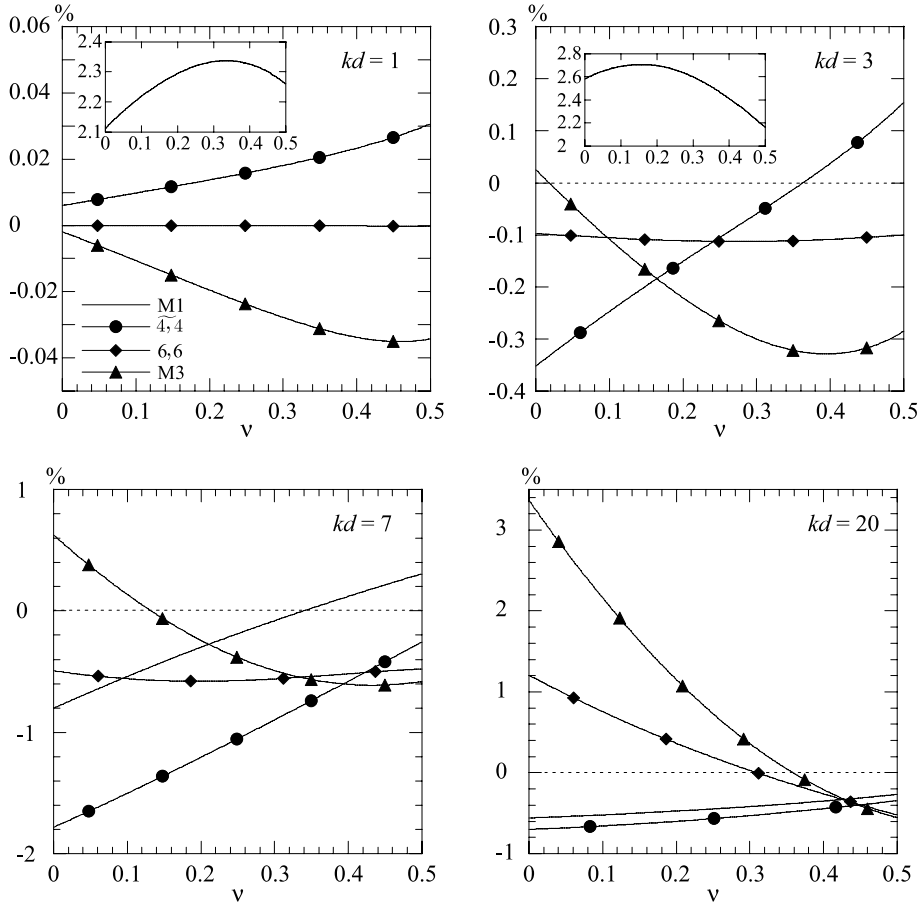

Fig. 3. Relative discrepancy $\left(v_{\mathrm{f}}^{(\mathrm{approx})} - v_{\mathrm{f}}^{(\mathrm{exact})}\right)/v_{\mathrm{f}}^{(\mathrm{exact})}$, in %, for different approximations of the flexural velocity v_{f} as a function of the Poisson's ratio in the cuts $kd = \mathrm{const}$. ($kd = 1, 3, 7, 20$). The curves' labels, indicated in the first plot, imply: M_1 is Mindlin's formula $(1)_1$; M_3 is $(1)_2$ optimized via (4); $\widetilde{4,4}$ is the modified Padé approximation with $N = 4$; 6,6 is the Padé approximation with $N = 6$.

M_1) improves the short-wave fitting compared to the 'standard' Padé. The second-order modified Padé approximation $v_{\mathrm{f}}(k) \approx \sqrt{[\widetilde{v}_{\mathrm{f}}^2(k)]_{4,4}}$ (the curve $\widetilde{4,4}$) improves the long-wave range accuracy of $(1)_1$ and betters the accuracy of Mindlin's formula with rotary inertia $(1)_2$ (the curve M_2), but falls behind a remarkably good precision of the optimized Mindlin's fit (labeled M_3) in the broad intermediate spectral interval. The differences, though, lie within quite a high (about 1% or better) approximation accuracy anyway. Besides, the short-wave plateau may indeed be estimated independently by c_{R} (or by (7), if higher precision is needed).

As it has been repeatedly pointed out in the literature, there hardly exists an 'unreservedly best' choice of the flexural velocity approximation in view of various criteria. The preference may hinge on a better precision for velocity fitting in a given spectral range, or accuracy of displacement–stress field estimation that is quite important for diffraction problems, or 'cost-efficiency' of computation, or suitability of explicit analytical representation of dispersion dependence for its plugging into further theoretical development involving integration. In this light, it is recalled that the Nth-order Padé approximant $[v_{\mathrm{f}}^2]_{N,N}$ or $[\widetilde{v}_{\mathrm{f}}^2]_{N,N}$ verifies the 'authentic' dispersion equation with the accuracy not worse than $(kd)^{2N}$ or $(kd)^{2N-2}$, respectively, hence

ensures this accuracy in recovering the through-plate wave field. The approximation of the squared velocity $v_f^2(k)$ is in the form of a fractional rational function (irrationality is avoided), whose computation requires knowledge of N Taylor coefficients of $v_f^2(k)$ or of $N-1$ coefficients and c_R.

The considerations, used above for the flexural-velocity fitting in free isotropic plates without appeal to the wave motion modelling, suggest straightforward 'heuristic' guidelines to be exercised for more general plate problems. This aspect is discussed in the next section.

4. Examples of generalization

4.1. Fluid-loaded plate

Consider the real velocity $v_A(k)$ of the flexural-type wave (A branch) in an isotropic plate immersed into non-viscous fluid with density ρ_w and speed of sound $c_w < c_R$. Bearing in mind the classical approximations by Osborne and Hart (1945) for the long-wave onset of the A branch,

$$v_A(k)|_{kd\ll 1} \approx \frac{\kappa(kd)^{3/2}}{\sqrt{kd+2\rho_w/\rho}} \tag{13}$$

and for the Scholte velocity c_{Sch}, which is the short wave limit of this branch, the overall approximation for $v_A(k)$ may be sought through the free-plate fitting formulas, modified by the following substitutions:

$$\kappa^2 \to \frac{\kappa^2 kd}{kd+2\rho_w/\rho}, \qquad c_R^2 \to c_{Sch}^2 \tag{14}$$

(ρ_w/ρ instead of $2\rho_w/\rho$ if the plate is loaded on one side only). For instance, applying (14) to Mindlin's relation $(1)_1$ and to the second-order modified Padé approximant ((11) with $N=4$) yields

$$\begin{aligned} v_A(k) &\approx \frac{\kappa kd}{\sqrt{1+2(\rho_w/\rho kd)+\left(\kappa^2/c_{Sch}^2\right)(kd)^2}}, \\ v_A(k) &\approx \frac{\kappa kd\sqrt{\widetilde{\alpha}_2^{(4,4)}+\widetilde{\alpha}_4^{(4,4)}(kd)^2}}{\sqrt{[1+(2\rho_w/\rho kd)]\left[\widetilde{\alpha}_2^{(4,4)}+\widetilde{\beta}_2^{(4,4)}(kd)^2\right]+\left(\kappa^2\widetilde{\alpha}_4^{(4,4)}/c_{Sch}^2\right)(kd)^4}}. \end{aligned} \tag{15}$$

Fig. 4 shows that the simple approximation $(15)_1$ works fairly well, except in the intermediate kd-range where it fails to emulate a sharp crossover of the exact curve from the ascending to the flat trend (the fitting improves for a relatively larger ρ_w/ρ, when this turn is smoother). The curve $(15)_2$ produces much better accuracy for long waves but then raises above c_w, which is incorrect physically, and hence it should rather be used up to its intersection with almost horizontal plateau and replaced by c_{Sch} afterward. Note that $(15)_2$ is actually not the Padé approximant of the dispersion in an immersed plate. Other estimations for the A branch may be put forward but we shall not delve into this problem here.

4.2. Anisotropic plate

4.2.1. Taylor series for $v_f^2(k)$

Consider a homogeneous anisotropic plate with the tensor of elastic coefficients c_{ijkl}. Denote by **m** and **n** the unit vectors parallel, respectively, to the propagation direction along the plate and to the normal to the plate faces. Recall the definition of the Stroh matrix

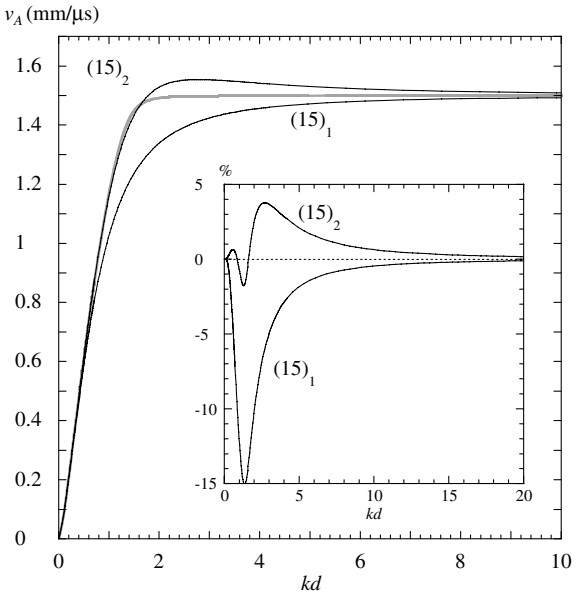

Fig. 4. Approximation of the A branch in a steel plate immersed in water. Thick gray line is the exact curve, thin black lines are the approximations by $(15)_1$ and $(15)_2$. The inset shows the relative discrepancy $\left(v_A^{(\text{approx})} - v_A^{(\text{exact})}\right)/v_A^{(\text{exact})}$.

$$\mathbf{N}(v) = \begin{pmatrix} \mathbf{N}_1 & \mathbf{N}_2 \\ \mathbf{N}_3 - \rho v^2 \mathbf{I} & \mathbf{N}_1^{\mathrm{T}} \end{pmatrix}; \quad \mathbf{N}_1 = -(nn)^{-1}(nm), \quad \mathbf{N}_2 = -(nn)^{-1}, \quad \mathbf{N}_3 = (mm) - (mn)(nn)^{-1}(nm), \tag{16}$$

where $(ab) \equiv a_i c_{ijkl} b_l$ with $\mathbf{a},\mathbf{b} = \mathbf{m}$ or $\mathbf{n}$; T denotes transpose, and $\mathbf{I}$ is the identity matrix (see Ting (1996) for explicit details, with the reservation that (16) differs from Ting's formulation by inverse signs of $\mathbf{N}_2$ and $\mathbf{N}_3$).

The plane-wave solution of the equation of motion may be written in the form of the 6×6 propagator $\mathbf{M} = \exp[\mathrm{i}kd\mathbf{N}(v^2)]$, then the dispersion equation for a traction-free plate is $\det[\mathbf{M}(v^2,k)]_3 = 0$, where the subscript 3 indicates the 3×3 left off-diagonal block of $\mathbf{M}$. The coefficients of Taylor series

$$v_{\mathrm{f}}^2(k) = \sum_{n=1}^{\infty} A_{2n}(kd)^{2n} \tag{17}$$

can be obtained by recursive solving of the dispersion equation with this series inserted

$$\det\left[\mathbf{M}(v_{\mathrm{f}}^2(k),k)\right]_3 = \det\left\{\sum_{n=1}^{\infty} \frac{(\mathrm{i}kd)^n}{n!}\left[\mathbf{N}^n(v_{\mathrm{f}}^2(k))\right]_3\right\} = \det\left[\mathrm{i}kd\sum_{n=0}^{\infty}\mathbf{\Delta}_n(kd)^n\right] = 0. \tag{18}$$

For any odd number N the matrix coefficient $\mathbf{\Delta}_N$ contains the sought-for Taylor coefficients A_{2n} up to $2n = N - 1$, and for even N it is $\mathbf{\Delta}_N = \mathbf{\Lambda}_N - A_N\mathbf{I}$ with $\mathbf{\Lambda}_N$ including A_{2n} up to $2n = N - 2$. Hence for any (even) N, given that A_{2n} for $2n < N$ are known, the coefficient A_N is found by computing the coefficient for a single term of the kd-series of $\det\left[\sum_{n=0}^{N}\mathbf{\Delta}_n(kd)^n\right]$—namely, for the term proportional to $(kd)^{3N}$ (or $(kd)^{2N}$ in the 2×2 in-plane case), and equating this coefficient to zero. Exactly the same procedure applies to the upper fundamental branches. It is valid for any anisotropic or isotropic materials (in fact, this is how the coefficients of series $(5)_1$, specifying (17) for isotropic plates, were obtained).

For a general anisotropic setting of the problem (none of the vectors **m**, **n** and **m** × **n** is a symmetry axis or a normal to a symmetry plane), the first two coefficients of the Taylor series (17) are[4]

$$A_2 = \kappa^2 = \frac{1}{12\rho}\mathbf{m}\cdot\mathbf{N}_3\mathbf{m}\ (>0),$$
$$A_4 = \frac{1}{(6!)\rho}\mathbf{m}\cdot(\mathbf{N}_1^{\mathrm{T}}\mathbf{N}_3\mathbf{N}_1 + 6\mathbf{N}_3\mathbf{N}_2\mathbf{N}_3 + 2\mathbf{N}_3\mathbf{N}_1^2 - 5\mathbf{N}_3\mathbf{N}_1\mathbf{q}\mathbf{N}_1\mathbf{N}_3 - 5\mathbf{N}_3)\mathbf{m}, \tag{19}$$

where **q** is the pseudoinverse to $\mathbf{N}_3$: $(\mathbf{q}\mathbf{N}_3)_{ij} = \delta_{ij} - n_i n_j$ (note that (19) is presented in a form independent of the reference base(s) for **m** and **N**). There is no principal difficulty in finding higher-order Taylor coefficients with the aid of symbolic-algebra software, however, for a general anisotropy they grow quite lengthy, especially when displayed directly in terms of c_{ijkl}. Some examples are presented in the Appendix C. Note that the value $(19)_1$ of the leading-order coefficient $A_2 = \kappa^2$ goes back to Lekhnitskii's theory (available in his book of 1968), which assumes the presence of a horizontal symmetry plane but, insofar as $(19)_1$ is concerned, this assumption is in fact redundant (see Shuvalov, 2000).

4.2.2. Padé approximation

Apart from relatively laborious calculation of the Taylor coefficients due to anisotropy, the Padé scheme remains straightforward and, being uninvolved with wave motion modelling, can readily be implemented for the flexural velocity in an arbitrary anisotropic plate. The Padé approximation is assuredly robust in the long wave range. At the same time, fitting the whole dispersion curve $v_{\mathrm{f}}(k)$ is efficient only if the curve is smooth enough. This may be not the case for an anisotropic plate. More specifically, the flexural velocity branch has a rippled shape of the Rayleigh plateau when the complex values of normal wave numbers $p_\alpha = k_{\mathbf{n}\alpha}/k$ of the partial evanescent modes $\alpha = 1,\ldots,6$ possess real parts (cf. 'isotropic' (7), where $\mathrm{Im}\,p = q$, $\mathrm{Re}\,p = 0$). In particular, $\mathrm{Re}\,p_\alpha \neq 0$ is typical in the absence of a horizontal symmetry plane. Roughly speaking, the more distorted the bulk-mode slowness sheets in the sagittal plane (**m**, **n**) are and the more they are misoriented relatively to the horizontal direction **m**, the greater the sample values of $\mathrm{Re}\,p_\alpha(v)$ for evanescent modes and hence the more pronounced the wavering of the fundamental branches along the short wave plateau. Interestingly, this is how the horizontal symmetry plane, which stipulates the model plate theories, comes into play in the present context of fitting the curve $v_{\mathrm{f}}(k)$: this plane absence is insignificant for implementation technicalities but it does affect the curve shape and hence the efficiency of fitting. Furthermore, it is well-known that the existence of a horizontal symmetry plane does not yet ensure a steady shape of the fundamental branches—provided the bulk-mode slowness sheets in the (**m**, **n**) plane have 'exposed' regions projecting on **m**, the fundamental velocity curves produce a weaving pattern with multiple intersections, which occur exactly at c_{R} if (**m**, **n**) is also a symmetry plane (Solie and Auld, 1973; Li and Thompson, 1990) or at some non-invariant points otherwise. (It is carefully noted that the geometry of bulk-mode slowness sheets cannot indeed fully predict the behaviour of complex *functions* $p_\alpha(v)$ in the subsonic velocity interval; for instance, a slowness sheet, which is convex but has small curvature at **m**, may precipitate a rippled Rayleigh plateau, particularly if c_{R} is well detached from the bulk-mode threshold.)

From this viewpoint, consider examples of the orthorhombic plate setting (the sagittal and boundary planes are symmetry planes) with the smooth flexural velocity branch and with its markedly rippled shape. Both cases may be represented by the tetragonal TeO_2 crystal, in which one of the principal cuts has convex slowness sheets and the other contains the slowness sheet with protruded diagonal 'whiskers' (e.g. Auld, 1973). Application of the Padé approximations is demonstrated in Fig. 5. Relevant explicit calculations

[4] The notation $A_2 = \kappa^2$ is kept in understanding that the value of the flexural-branch slope κ depends on the symmetry and simplifies to (2) for the isotropic setting.

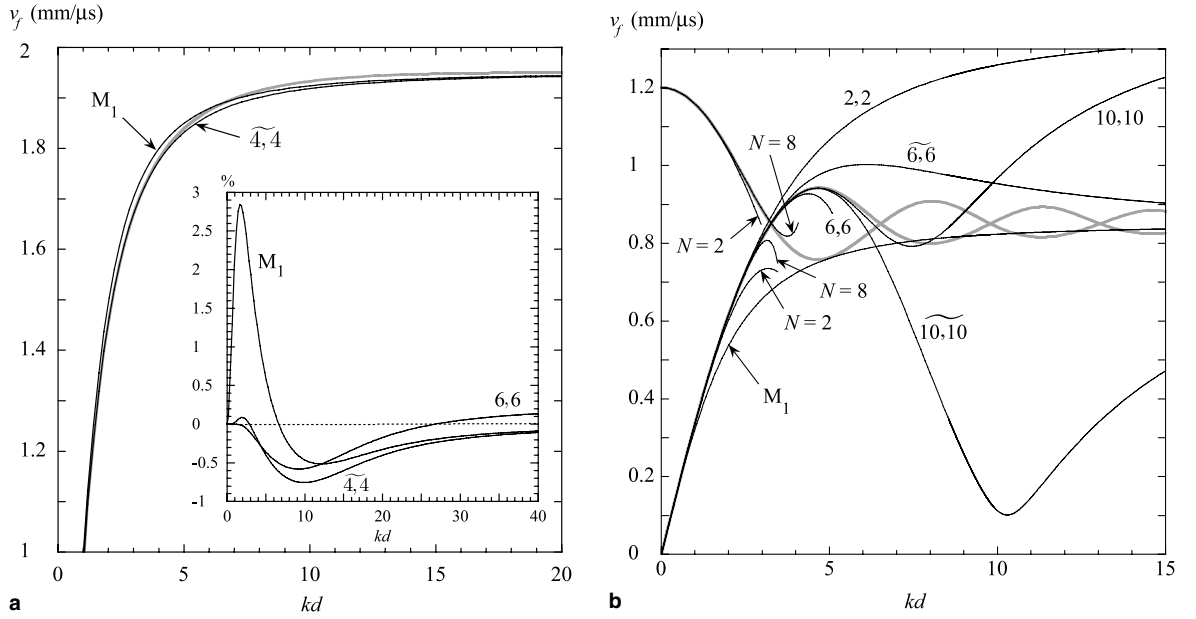

Fig. 5. Approximation of the flexural branch in the orthorhombic plates, which are cut from the TeO_2 crystal (the material constants are taken from Auld's (1973) book). (a) The sagittal plane $(\mathbf{m},\mathbf{n})$ is XZ and the propagation direction $\mathbf{m}$ is Z; (b) $(\mathbf{m},\mathbf{n})$ is XY and $\mathbf{m}$ is X or Y (here X, Y, Z are the crystallographic axes). Thick gray line shows the exact flexural and (in Fig. b) S_0 branches. Thin black lines are the fits by $(1)_1$ with $\kappa^2 = \frac{1}{12\rho}\left(c_{11} - \frac{c_{12}^2}{c_{22}}\right)$ (labeled M_1), by the Taylor series truncated by the term $\sim(kd)^{2N}$ inclusive (labeled by N); by the Padé $[v_f^2]_{N,N}$ and modified Padé $[\widetilde{v_f^2}]_{N,N}$ approximants (labeled N,N and $\widetilde{N,N}$, respectively). Inset to (a) shows the relative discrepancy $(v_f^{(\mathrm{approx})} - v_f^{(\mathrm{exact})})/v_f^{(\mathrm{exact})}$.

are outlined in the Appendices B and C.3. Recall that the first order of the modified Padé scheme, enforcing the Rayleigh limit c_R, is Mindlin's formula $(1)_1$ with 'anisotropic' κ.

Fig. 5a confirms the accuracy of the approximations of the full extent of anisotropic-plate flexural branch $v_f(k)$ once its short wave plateau is smooth. In this case, there is not much difference in the fitting efficiency compared to isotropic plates (this observation applies as well to other approximations displayed in Figs. 1–3 and not plotted in Fig. 5a). Otherwise, as shown in Fig. 5b, fitting is worthwhile only for the relatively long-wave range. At the same time, it is seen that a good fit for the steadily ascending part of the flexural branch (up to $kd \lesssim 4$, that is $fd \lesssim 3.5$ MHz · mm, in Fig. 5b) is achievable by the low-order Padé approximation (see 2,2-curve), and that the higher-order approximants are capable of 'capturing' the formation of rippled shape of the branch. Note also that the flexural branch in Fig. 5b admits a better long-wave fit by the truncated Taylor series than in the case of steel plate, see Fig. 1.

4.3. Transversely inhomogeneous plate

The same guidelines can be applied for fitting the flexural velocity $v_f(k)$ in inhomogeneous plates, whose material properties arbitrary vary along the direction normal to plate faces. On replacing the power series of exponential of the Stroh matrix $\mathbf{N}$ by the Peano expansion (whereby multiple integrals of $\mathbf{N}$ appear in place of its powers), the recursive procedure for finding the coefficients of $v_f^2(k)$ Taylor series (17) remains the same as for homogeneous plates. On the other hand, the flexural branch shape now depends essentially on the local features of the inhomogeneity profile. The short wave mold may incorporate different trends and plateaus even for isotropic plate materials. Thus, as in the previously discussed case of anisotropic

homogeneous plates, although for different reasons, the efficiency of the Padé approximation should generally be restricted to the long wave range. Bearing this in mind, we however opted to mention the 'favourable' example of a relatively steady flexural curve, which comes about for uniform variation of material properties. Let us confine attention to the simple case of isotropic plate. The leading-order Taylor coefficient $A_2 = \kappa^2$ for $v_f^2(k)$ (squared slope of $v_f(k)$) in an inhomogeneous isotropic plate is

$$\kappa^2 = \frac{4}{\int_0^1 \rho(\zeta)\,\mathrm{d}\zeta \int_0^1 \varphi(\zeta)\,\mathrm{d}\zeta} \int_0^1 \int_0^\zeta (\zeta - \zeta_1)^2 \varphi(\zeta)\varphi(\zeta_1)\mathrm{d}\zeta\,\mathrm{d}\zeta_1 \quad \text{with } \varphi(\zeta) = \rho(\zeta)c_t^2(\zeta)\left(1 - \frac{c_t^2(\zeta)}{c_l^2(\zeta)}\right), \tag{20}$$

where $c_{l,t}(\zeta)$ are the velocities of longitudinal and transverse bulk modes, $\zeta \in [0,1]$ is dimensionless through-plate coordinate (Shuvalov et al., 2005). We assume that the plate composition transforms in a linear fashion from pure titanium on one face to pure α-titanium on the other, so that the velocity profile $c_{l,t}(\zeta)$ varies linearly from the titanium data ($c_l(0) = 6.06$, $c_t(0) = 3.23$ mm/μs) to that of α-titanium ($c_l(1) = 6.66$, $c_t(1) = 3.553$ mm/μs) while density is constant ($\rho = 4.46$ g/cm^3). Fig. 6 shows that already Mindlin's formula $(1)_1$ with $\kappa = 1.654$ mm/μs obtained from (20) and with $c_R = c_R(0) = 2.994$ mm/μs ('homogeneous' value referred to the 'slow' plate face) supplies a satisfactory fit for the full extent of the flexural velocity branch.

Returning to the case of fluid loading, it is noted that the long-wave estimation (13) remains valid for anisotropic and/or inhomogeneous materials (see Shuvalov, 2002; Shuvalov et al., 2005) and therefore, Eq. (15) with appropriate κ^2 and c_{Sch}^2 can be used for approximating the A velocity branch in anisotropic inhomogeneous plates immersed in fluid. To this end, advantageous is the fact that the speed of sound in fluid c_w is usually notably smaller than the Rayleigh velocity in crystals (in this regard, low c_R in Fig. 5b is rather an exception than a norm) and than velocity of high-frequency channels in inhomogeneous materi-

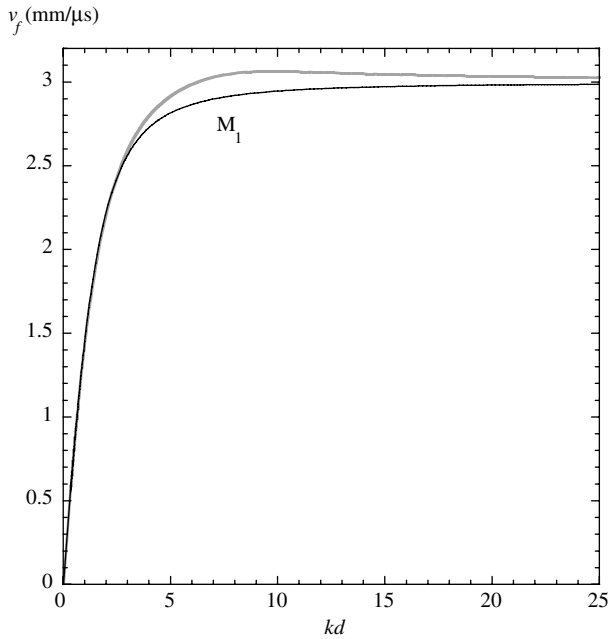

Fig. 6. Approximation of the flexural branch in the isotropic plate with a linear variation of material properties across the plate. Thick gray line is the exact curve, thin black line is fitting by Mindlin's $(1)_1$ with κ given by (20).

als. In consequence, those factors, which distort the flexural-branch shape and thereby inhibit the Padé fitting of the whole branch in free plates, are less likely to intervene in the case of the A branch in fluid-loaded plates.

Acknowledgements

The authors are grateful to G.A. Rogerson for the helpful comments to the manuscript, and to C. Baron for making the numerical calculations used in Fig. 6.

Appendix A. The higher-order coefficients a_{2n} in the Taylor series $(5)_1$ for $v_f^2(k)$ in isotropic plate

$$\begin{aligned}
a_{10} &= 5110v^4 - 110,090v^3 + 584,257v^2 - 1,059,940v + 602,410,\\
a_{12} &= \frac{1}{35}(282,895v^5 - 90,572,134v^4 + 754,982,390v^3 - 2,386,810,276v^2\\
&\quad + 3,109,098,177v - 1,404,361,931),\\
a_{14} &= \frac{1}{2}(3,440,220v^6 - 153,108,900v^5 + 1,840,593,186v^4 - 8,868,547,040v^3\\
&\quad + 19,607,784,669v^2 - 19,849,038,802v + 7,437,643,415),\\
a_{16} &= \frac{2}{15}(355,554,717v^7 - 20,978,379,363v^6 + 343,393,156,317v^5 - 2,332,360,918,791v^4\\
&\quad + 7,695,401,450,679v^3 - 12,978,692,736,341v^2 + 10,724,754,208,055v - 3,433,209,020,623).
\end{aligned} \tag{21}$$

Appendix B. The coefficients of the Padé approximants for $v_f^2(k)$

Assuming arbitrary anisotropy and referring to the Taylor series in the form $v_f^2(k) = \sum_{n=1}^{\infty} A_{2n}(kd)^{2n}$, we seek the coefficients of the Padé and modified Padé approximants

$$\begin{aligned}
\left[v_f^2(k)\right]_{N,N} &= \frac{\Gamma_2^{(N,N)}(kd)^2 + \cdots + \Gamma_N^{(N,N)}(kd)^N}{\beta_0^{(N,N)} + \beta_2^{(N,N)}(kd)^2 + \cdots + \beta_N^{(N,N)}(kd)^N} \quad \left(\Gamma_2^{(N,N)} = A_2\beta_0^{(N,N)}\right),\\
\left[\widetilde{v}_f^2(k)\right]_{N,N} &= \frac{\widetilde{\Gamma}_2^{(N,N)}(kd)^2 + \cdots + \widetilde{\Gamma}_N^{(N,N)}(kd)^N}{\widetilde{\beta}_0^{(N,N)} + \widetilde{\beta}_2^{(N,N)}(kd)^2 + \ldots + \left(\widetilde{\Gamma}_N^{(N,N)}\Big/c_R^2\right)(kd)^N} \quad \left(\widetilde{\Gamma}_2^{(N,N)} = A_2\widetilde{\beta}_0^{(N,N)}\right),
\end{aligned} \tag{22}$$

(where N is even) in terms of the Taylor coefficients A_{2n}. The coefficients for $[v_f^2]_{N,N}$ and $[\widetilde{v}_f^2]_{N,N}$ up to $N = 6$ are, respectively, as follows:

$$\begin{aligned}
N = 2:&\quad \Gamma_2^{(2,2)} = A_2^2, \quad \beta_2^{(2,2)} = -A_4;\\
N = 4:&\quad \Gamma_2^{(4,4)} = A_2(A_2A_6 - A_4^2), \quad \Gamma_4^{(4,4)} = 2A_2A_4A_6 - A_2^2A_8 - A_4^3,\\
&\quad \beta_2^{(4,4)} = A_4A_6 - A_2A_8, \quad \beta_4^{(4,4)} = A_4A_8 - A_6^2;
\end{aligned}$$

$$
\begin{aligned}
N=6:\quad \Gamma_2^{(6,6)} &= A_2(A_2A_6A_{10}+2A_4A_6A_8-A_2A_8^2-A_4^2A_{10}-A_6^3),\\
\Gamma_4^{(6,6)} &= A_2^2A_8A_{10}+A_2A_6^2A_8+A_2A_4^2A_{12}+2A_4^2A_6A_8-A_2^2A_6A_{12}-A_4A_6^3-A_4^3A_{10}-2A_2A_4A_8^2,\\
\Gamma_6^{(6,6)} &= A_4^3A_{12}+A_2^2A_8A_{12}+2A_2A_6^2A_{10}+3A_4A_6^2A_8+2A_2A_4A_8A_{10}-A_2^2A_{10}^2-2A_2A_4A_6A_{12}\\
&\quad -A_6^4-A_4^2A_8^2-2A_2A_6A_8^2-2A_4^2A_6A_{10},\\
\beta_2^{(6,6)} &= A_4^2A_{12}+A_6^2A_8+A_2A_8A_{10}-A_4A_8^2-A_2A_6A_{12}-A_4A_6A_{10},\\
\beta_4^{(6,6)} &= A_6^2A_{10}+A_2A_8A_{12}+A_4A_8A_{10}-A_2A_{10}^2-A_6A_8^2-A_4A_6A_{12},\\
\beta_6^{(6,6)} &= A_8^3+A_4A_{10}^2+A_6^2A_{12}-A_4A_8A_{12}-2A_6A_8A_{10};
\end{aligned}
\tag{23}
$$

$$
\begin{aligned}
N=2:\quad \widetilde{\Gamma}_2^{(2,2)} &= A_2^2;\\
N=4:\quad \widetilde{\Gamma}_2^{(4,4)} &= A_2^2(A_2^2+c_R^2A_4),\quad \widetilde{\Gamma}_4^{(4,4)} = A_2c_R^2(A_4^2-A_2A_6),\quad \widetilde{\beta}_2^{(4,4)} = -A_2(A_2A_4+c_R^2A_6);\\
N=6:\quad \widetilde{\Gamma}_2^{(6,6)} &= A_2(A_4^3+A_2^2A_8-2A_2A_4A_6+c_R^2A_4A_8-c_R^2A_6^2),\\
\widetilde{\Gamma}_4^{(6,6)} &= A_4^4+A_2^2A_6^2+2A_2^2A_4A_8-3A_2A_4^2A_6-A_2^3A_{10}+c_R^2(A_4^2A_8+A_2A_6A_8-A_4A_6^2-A_2A_4A_{10}),\\
\widetilde{\Gamma}_6^{(6,6)} &= c_R^2(A_2A_6A_{10}+2A_4A_6A_8-A_6^3-A_2A_8^2-A_4^2A_{10}),\\
\widetilde{\beta}_2^{(6,6)} &= A_2A_6^2+A_2A_4A_8-A_2^2A_{10}-A_4^2A_6+c_R^2(A_6A_8-A_4A_{10}),\\
\widetilde{\beta}_4^{(6,6)} &= A_4A_6^2+A_2A_4A_{10}-A_4^2A_8-A_2A_6A_8+c_R^2(A_6A_{10}-A_8^2).
\end{aligned}
\tag{24}
$$

As noted in Appendix C.3, for the orthorhombic and higher symmetry settings of the problem all the Taylor coefficients A_{2n} are proportional to the leading-order one $A_2=\kappa^2$, hence so are all the Padé approximants. In this case, denoting the numerator coefficients in (22) by $\Gamma_{2n}^{(N,N)}=\kappa^2\alpha_{2n}^{(N,N)}$ and $\widetilde{\Gamma}_{2n}^{(N,N)}=\kappa^2\widetilde{\alpha}_{2n}^{(N,N)}$ leads to (10) and (12).

Appendix C. Examples of the Taylor coefficients for squared fundamental velocities in anisotropic plate

Keeping the notation $v_f^2(k)=\sum_{n=1}^{\infty}A_{2n}(kd)^{2n}$ for the flexural branch, denote the Taylor series for the upper fundamental branches, labeled S_{01} and S_{02}, by $v_{S_{0\alpha}}^2(k)=\sum_{n=0}^{\infty}A_{2n}^{(S_{0\alpha})}(kd)^{2n}$. Once coefficients A_{2n} and $A_{2n}^{(S_{0\alpha})}$ are obtained, the same number of coefficients of the power series for $v^2(\omega)$ and $v(k)$, $v(\omega)$ follow from standard formulas operating on power series. It is noted that those relations, which are given below in terms of quadratic forms of blocks of the Stroh matrix $\mathbf{N}$ (16), are invariant indeed with respect to the choice of coordinate system(s) for involved objects. For all the formulas detailed in terms of elastic coefficients c_{ijkl}, the reference basis $\{X_1,X_2,X_3\}$ is specified as $\{X_1,X_2,X_3\}=\{\mathbf{m},\mathbf{n},\mathbf{t}\}$, where $\mathbf{t}=\mathbf{m}\times\mathbf{n}$.

C.1. A symmetry plane parallel to the boundary plane ($\mathbf{m},\mathbf{t}$) = X_1X_3

In this case, the Stroh-matrix blocks referred to the basis $\{X_1,X_2,X_3\}=\{\mathbf{m},\mathbf{n},\mathbf{t}\}$ are

$$
\mathbf{N}_1=\begin{pmatrix} 0 & -1 & 0\\ -\dfrac{c_{12}}{c_{22}} & 0 & -\dfrac{c_{25}}{c_{22}}\\ 0 & 0 & 0\end{pmatrix},\quad
\mathbf{N}_2=\frac{1}{\Delta_{46}}\begin{pmatrix} -c_{44} & 0 & c_{46}\\ 0 & -\dfrac{\Delta_{46}}{c_{22}} & 0\\ c_{46} & 0 & -c_{66}\end{pmatrix},\quad
\mathbf{N}_3=\begin{pmatrix} c_{11}-\dfrac{c_{12}^2}{c_{22}} & 0 & c_{15}-\dfrac{c_{12}c_{25}}{c_{22}}\\ 0 & 0 & 0\\ c_{15}-\dfrac{c_{12}c_{25}}{c_{22}} & 0 & c_{55}-\dfrac{c_{25}^2}{c_{22}}\end{pmatrix},
\tag{25}
$$

where $\Delta_{46} = c_{44}c_{66} - c_{46}^2$ (> 0). The Taylor coefficients (19) for $v_\Gamma^2(k)$ become

$$\begin{aligned} A_2 &= \frac{1}{12\rho}\mathbf{m}\cdot\mathbf{N}_3\mathbf{m} = \frac{1}{12\rho}\left(c_{11} - \frac{c_{12}^2}{c_{22}}\right), \\ A_4 &= \frac{1}{(6!)\rho}\left[6\mathbf{m}\cdot\mathbf{N}_3\mathbf{N}_2\mathbf{N}_3\mathbf{m} - (\mathbf{m}\cdot\mathbf{N}_3\mathbf{m})(5 + 2\mathbf{n}\cdot\mathbf{N}_1\mathbf{m})\right] \end{aligned} \tag{26}$$

(note that A_4 is not proportional to $\mathbf{m}\cdot\mathbf{N}_3\mathbf{m}$). The leading-order coefficients for the upper fundamental branches are

$$\begin{aligned} &A_0^{(S_{0\alpha})} = \frac{\eta_\alpha}{\rho},\ A_2^{(S_{0\alpha})} = -\frac{\eta_\alpha}{12\rho}(\mathbf{n}\cdot\mathbf{N}_1\mathbf{e}_\alpha)^2, \\ &A_4^{(S_{0\alpha})} = \frac{1}{(6!)\rho}(\mathbf{n}\cdot\mathbf{N}_1\mathbf{e}_\alpha)^2\left\{6\eta_\alpha^2\mathbf{n}\cdot\mathbf{N}_2\mathbf{n} - (\eta_\alpha - \eta_\beta)(\mathbf{e}_\beta\cdot\mathbf{m})^2 + \eta_\alpha\left[2\mathbf{n}\cdot\mathbf{N}_1\mathbf{m} + 5(\mathbf{n}\cdot\mathbf{N}_1\mathbf{e}_\alpha)^2 + \frac{5\eta_\alpha}{\eta_\alpha - \eta_\beta}(\mathbf{n}\cdot\mathbf{N}_1\mathbf{e}_\beta)^2\right]\right\}, \\ &\qquad \alpha \neq \beta = 1,2, \end{aligned} \tag{27}$$

where $\eta_{1,2}$ and $\mathbf{e}_{1,2}$ are the nonzero eigenvalues and corresponding unit-normalized eigenvectors of $\mathbf{N}_3$.

C.2. A symmetry plane parallel to the sagittal plane $(\mathbf{m}, \mathbf{n}) = X_1X_2$

The 2×2 matrices, induced in this case by the Stroh-matrix blocks in X_1X_2, are

$$\begin{aligned} \mathbf{N}_1 &= \begin{pmatrix} \frac{1}{\Delta_{26}}(c_{12}c_{26} - c_{16}c_{22}) & -1 \\ \frac{1}{\Delta_{26}}(c_{16}c_{26} - c_{12}c_{66}) & 0 \end{pmatrix}, \quad \mathbf{N}_2 = \frac{1}{\Delta_{26}}\begin{pmatrix} -c_{22} & c_{26} \\ c_{26} & -c_{66} \end{pmatrix}, \\ \mathbf{N}_3 &= \begin{pmatrix} c_{11} - \frac{1}{\Delta_{26}}(c_{22}c_{16}^2 - 2c_{12}c_{16}c_{26} + c_{12}^2c_{66}) & 0 \\ 0 & 0 \end{pmatrix}, \end{aligned} \tag{28}$$

where $\Delta_{26} = c_{22}c_{66} - c_{26}^2$ (> 0). The coefficients (19) for $v_\Gamma^2(k)$ take the form

$$\begin{aligned} A_2 &= \frac{1}{12\rho}\mathbf{m}\cdot\mathbf{N}_3\mathbf{m} = \frac{1}{12\rho}\left(c_{11} - \frac{c_{22}c_{16}^2 - 2c_{12}c_{16}c_{26} + c_{12}^2c_{66}}{\Delta_{26}}\right), \\ A_4 &= \frac{1}{(6!)\rho}(\mathbf{m}\cdot\mathbf{N}_3\mathbf{m})\Big[6(\mathbf{m}\cdot\mathbf{N}_3\mathbf{m})(\mathbf{m}\cdot\mathbf{N}_2\mathbf{m}) - 2(\mathbf{m}\cdot\mathbf{N}_1\mathbf{m})^2 - 2\mathbf{n}\cdot\mathbf{N}_1\mathbf{m} - 5\Big]. \end{aligned} \tag{29}$$

The leading-order Taylor coefficients for the squared velocity $v_{S_0}^2(k)$ of the upper in-plane fundamental branch, labeled S_0 (in understanding, though, that it is *not* symmetric in the absence of a horizontal symmetry plane), are

$$\begin{aligned} A_0^{(S_0)} &= \frac{1}{\rho}\mathbf{m}\cdot\mathbf{N}_3\mathbf{m}, \\ A_2^{(S_0)} &= -\frac{1}{12\rho}(\mathbf{m}\cdot\mathbf{N}_3\mathbf{m})(\mathbf{n}\cdot\mathbf{N}_1\mathbf{m})^2, \\ A_4^{(S_0)} &= \frac{1}{(6!)\rho}(\mathbf{m}\cdot\mathbf{N}_3\mathbf{m})(\mathbf{n}\cdot\mathbf{N}_1\mathbf{m})^2\Big[6(\mathbf{m}\cdot\mathbf{N}_3\mathbf{m})(\mathbf{n}\cdot\mathbf{N}_2\mathbf{n}) + 2(\mathbf{m}\cdot\mathbf{N}_1\mathbf{m})^2 + (\mathbf{n}\cdot\mathbf{N}_1\mathbf{m})(5\mathbf{n}\cdot\mathbf{N}_1\mathbf{m} + 2)\Big], \end{aligned} \tag{30}$$

where $\mathbf{m}$ and $\mathbf{m}\cdot\mathbf{N}_3\mathbf{m}$ are, in this case, the eigenvector and eigenvalue of $\mathbf{N}_3$.

Interestingly, the assumption of the sagittal plane coinciding with a symmetry plane suffices for all the Taylor coefficients of $v_{\mathrm{f}}^2(k)$ and $v_{S_0}^2(k)$ to be proportional to $\mathbf{m}\cdot\mathbf{N}_3\mathbf{m}$ ($=12\rho\kappa^2$), that is, both in-plane fundamental velocities for a monoclinic plate in this setting are proportional to κ (obviously $\kappa\to 0$ leads to $v_{\mathrm{f},S_0}(k)\to 0$ and $c_{\mathrm{R}}\to 0$). On top of that, for $v_{S_0}^2(k)$ all the coefficients $A_{2n}^{(S_0)}$ with $n>0$ are in fact proportional to $\kappa^2(\mathbf{n}\cdot\mathbf{N}_1\mathbf{m})^2$, so that the upper fundamental branch at $\mathbf{n}\cdot\mathbf{N}_1\mathbf{m}=0$ is non-dispersive: $v_{S_0}=\left(\frac{1}{\rho}\mathbf{m}\cdot\mathbf{N}_3\mathbf{m}\right)^{1/2}$ for any k. Indeed, for the symmetry in hand, $-\mathbf{n}\cdot\mathbf{N}_1\mathbf{m}$ is equal to the Poisson's ratio $\nu(\mathbf{m},\mathbf{n})$ ($=s_{12}/s_{11}$ for $X_1\|\mathbf{m}$, $X_2\|\mathbf{n}$).

C.3. Symmetry planes parallel to the boundary and to the sagittal plane

Conjunction of the two preceding symmetry settings leads to the evident explicit simplifications. In particular, recall that the components of elasticity tensor c_{ijkl} with three among indices are not involved into the in-plane motion. The first six Taylor coefficients for $v_{\mathrm{f}}^2(k)$ specify in terms of elastic constants as follows:

$$
\begin{aligned}
A_2 &= \frac{C}{12\rho},\quad A_4 = -\frac{C}{(6!)\rho}\left(6\frac{C}{c_{66}}-2\frac{c_{12}}{c_{22}}+5\right),\\
A_6 &= \frac{2C}{3(8!)\rho}\left[51\frac{C^2}{c_{66}^2}+2\frac{C}{c_{66}}\left(63-18\frac{c_{12}}{c_{22}}-\frac{c_{66}}{c_{22}}\right)-28\frac{c_{12}}{c_{22}}-\frac{c_{12}^2}{c_{22}^2}+35\right],\\
A_8 &= -\frac{C}{(10!)\rho}\left[310\frac{C^3}{c_{66}^3}+2\frac{C^2}{c_{66}^2}\left(762-168\frac{c_{12}}{c_{22}}-13\frac{c_{66}}{c_{22}}\right)\right.\\
&\quad\left.+2\frac{C}{c_{66}}\left(630-396\frac{c_{12}}{c_{22}}-15\frac{c_{66}}{c_{22}}-7\frac{c_{12}^2}{c_{22}^2}-4\frac{c_{66}c_{12}}{c_{22}^2}\right)+175-210\frac{c_{12}}{c_{22}}+18\frac{c_{12}^2}{c_{22}^2}+22\frac{c_{12}^3}{c_{22}^3}\right],\\
A_{10} &= \frac{C}{(12!)\rho}\left[4146\frac{C^4}{c_{66}^4}+8\frac{C^3}{c_{66}^3}\left(4235-758\frac{c_{12}}{c_{22}}-67\frac{c_{66}}{c_{22}}\right)\right.\\
&\quad+\frac{C^2}{c_{66}^2}\left(55,770-28,776\frac{c_{12}}{c_{22}}-1672\frac{c_{66}}{c_{22}}-329\frac{c_{12}^2}{c_{22}^2}-23\frac{c_{66}^2}{c_{22}^2}-364\frac{c_{66}c_{12}}{c_{22}^2}\right)\\
&\quad+4\frac{C}{c_{66}}\left(5775-5742\frac{c_{12}}{c_{22}}-165\frac{c_{66}}{c_{22}}+429\frac{c_{12}^2}{c_{22}^2}-33\frac{c_{66}c_{12}}{c_{22}^2}\right.\\
&\quad\left.\left.+335\frac{c_{12}^3}{c_{22}^3}+41\frac{c_{12}^2c_{66}}{c_{22}^3}\right)+1925-3080\frac{c_{12}}{c_{22}}+759\frac{c_{12}^2}{c_{22}^2}+528\frac{c_{12}^3}{c_{22}^3}-126\frac{c_{12}^4}{c_{22}^4}\right],\\
A_{12} &= -\frac{C}{2(15!)\rho}\left[2,293,620\frac{C^5}{c_{66}^5}+5\frac{C^4}{c_{66}^4}\left(5,613,777-844,722\frac{c_{12}}{c_{22}}-80,182\frac{c_{66}}{c_{22}}\right)+2\frac{C^3}{c_{66}^3}\right.\\
&\quad\times\left(38,393,355-16,776,240\frac{c_{12}}{c_{22}}-1,182,415\frac{c_{66}}{c_{22}}-141,355\frac{c_{12}^2}{c_{22}^2}-216,168\frac{c_{12}c_{66}}{c_{22}^2}-20,521\frac{c_{66}^2}{c_{22}^2}\right)\\
&\quad+4\frac{C^2}{c_{66}^2}\left(15,840,825-13,423,410\frac{c_{12}}{c_{22}}-625,625\frac{c_{66}}{c_{22}}+865,748\frac{c_{12}^2}{c_{22}^2}-110,136\frac{c_{12}c_{66}}{c_{22}^2}-9035\frac{c_{66}^2}{c_{22}^2}\right.\\
&\quad\left.+2451\frac{c_{12}c_{66}^2}{c_{22}^3}+99,278\frac{c_{12}^2c_{66}}{c_{22}^3}+502,173\frac{c_{12}^3}{c_{22}^3}\right)+2\frac{C}{c_{66}}\left(7,882,875-10,810,800\frac{c_{12}}{c_{22}}-250,250\frac{c_{66}}{c_{22}}\right.\\
&\quad+2,276,274\frac{c_{12}^2}{c_{22}^2}+1,193,400\frac{c_{12}^3}{c_{22}^3}+138,099\frac{c_{12}^2c_{66}}{c_{22}^3}-208,918\frac{c_{12}^4}{c_{22}^4}-3080\frac{c_{12}^3c_{66}}{c_{22}^4}\Big)\\
&\quad\left.+875,875-1,751,750\frac{c_{12}}{c_{22}}+740,740\frac{c_{12}^2}{c_{22}^2}+334,334\frac{c_{12}^3}{c_{22}^3}-202,033\frac{c_{12}^4}{c_{22}^4}+3044\frac{c_{12}^5}{c_{22}^5}\right],
\end{aligned}
\tag{31}
$$

where $C = c_{11} - c_{12}^2/c_{22}$ ($= \mathbf{m}\cdot\mathbf{N}_3\mathbf{m} = 12\rho\kappa^2$). The first five coefficients for the Taylor series of the S_0 branch are

$$
\begin{aligned}
A_0^{(S_0)} &= \frac{C}{\rho}, \quad A_2^{(S_0)} = -\frac{C}{12\rho}\frac{c_{12}^2}{c_{22}^2}, \quad A_4^{(S_0)} = \frac{C}{(6!)\rho}\frac{c_{12}^2}{c_{22}^2}\left(-6\frac{c_{11}}{c_{22}} - 2\frac{c_{12}}{c_{22}} + 11\frac{c_{12}^2}{c_{22}^2}\right),\\
A_6^{(S_0)} &= -\frac{2C}{3(8!)\rho}\frac{c_{12}^2}{c_{22}^2}\left(51\frac{c_{11}^2}{c_{22}^2} + 36\frac{c_{11}c_{12}}{c_{22}^2} - \frac{c_{12}^2}{c_{22}^2} + 2\frac{c_{11}c_{12}^2}{c_{22}^2c_{66}} - 228\frac{c_{11}c_{12}^2}{c_{22}^3} - 64\frac{c_{12}^3}{c_{22}^3} + 212\frac{c_{12}^4}{c_{22}^4} - 2\frac{c_{12}^4}{c_{22}^3c_{66}}\right),\\
A_8^{(S_0)} &= -\frac{C}{(10!)\rho}\frac{c_{12}^2}{c_{22}^2}\left(310\frac{c_{11}^3}{c_{22}^3} + 336\frac{c_{11}^2c_{12}}{c_{22}^3} - 14\frac{c_{11}c_{12}^2}{c_{22}^3} - 22\frac{c_{12}^3}{c_{22}^3} + 26\frac{c_{11}^2c_{12}^2}{c_{22}^3c_{66}} - 2454\frac{c_{11}^2c_{12}^2}{c_{22}^4} - 8\frac{c_{11}c_{12}^3}{c_{22}^3c_{66}}\right.\\
&\quad \left. -1464\frac{c_{11}c_{12}^3}{c_{22}^4} - 4\frac{c_{12}^4}{c_{22}^4} - 82\frac{c_{11}c_{12}^4}{c_{22}^4c_{66}} + 5238\frac{c_{11}c_{12}^4}{c_{22}^5} + 8\frac{c_{12}^5}{c_{22}^4c_{66}} + 1338\frac{c_{12}^5}{c_{22}^5} + 56\frac{c_{12}^6}{c_{22}^5c_{66}} - 3269\frac{c_{12}^6}{c_{22}^6}\right).
\end{aligned}
\tag{32}
$$

It is noted that the sign of second derivative for the flexural velocity $v_f(k)$ at $k = 0$ (hence for $v_f(\omega)$ at $\omega = 0$), given by the sign of A_4, is negative as a rule, however, it is not always so unless the symmetry is high enough. For the orthorhombic setting under consideration, appealing to (31) shows that a convex onset of $v_f(k)$ (negative second derivative, $A_4 < 0$) is ensured if $c_{12} < \frac{5}{2}c_{22}$ ($\Rightarrow c_{11} < \frac{25}{4}c_{22}$), which is normally the case; but there is a concavity, if this inequality is inverse and c_{12}/c_{22} and/or c_{66}/c_{11} are large enough. The concavity condition is, though, quite stringent, and the concavity itself must be almost 'flat', so it is more reasonable to talk about an extended horizontal onset of $v_f(k)$ at small A_4. Evidently, $v_f(k)$ is always convex once there is, at least, a four-fold symmetry axis orthogonal to the sagittal plane (**m**, **n**). For the S_0 in-plane branch, the sign of second derivative v''_{S_0} in k or ω at the origin point is also usually negative though not always (besides, the signs of v''_{S_0} in k and ω may differ). By (32), positive $v''_{S_0}(k)$ at $k = 0$ occurs, e.g., for the TeO_2 plate with **n** parallel to the four-fold symmetry axis (the geometry used for Fig. 5b). Its positive value remains a possibility even for isotropic plates, whereas positive $v''_{S_0}(\omega)$ at $\omega = 0$ is ruled out once the vectors **m**, **n**, **t** are parallel to the four-fold symmetry axes (cubic plates).

References

Achenbach, J.D., 1973. Wave Propagation in Elastic Solids. North-Holland, Amsterdam.

Altenbach, H., 2000. On the determination of transverse shesr stiffness of orthotropic plates. Zeitschrift für angewandte mathematik und physik 51, 629–649.

Auld, B.A., 1973. Acoustic Fields and Waves in Solids, vol. 1. Wiley-Interscience Publication, New York.

Baker Jr., G.A., Graves-Morris, P., 1996. Padé Approximants. University Press Cambridge, Cambridge.

Destrade, M., 2003. Rayleigh waves in symmetry planes of crystals: explicit secular equations and some explicit wave speeds. Mechanics of Materials 35, 931–939.

Goldenveizer, A.L., Kaplunov, J.D., Nolde, E.V., 1990. Asymptotic analysis and improvements of Timoshenko–Reissner-type theories of plates and shells. Mechanics of Solids 25, 126–139.

Goldenveizer, A.L., Kaplunov, J.D., Nolde, E.V., 1993. On Timoshenko–Reissner type theories of plates and shells. International Journal of Solids and Structures 30, 675–694.

Graff, K.F., 1991. Wave Motion in Elastic Solids. Dover Publications, New York.

Jemielita, G., 1990. On kinematical assumptions of refined theories of plates: a survey. ASME Journal of Applied Mechanics 57, 1088–1091.

Kaplunov, Yu.D., Kossovich, L.Yu., 2004. Asymptotic model of Rayleigh waves in the far-field zone in an elastic half-plane. Doklady Physics 49, 234–236.

Kaplunov, J.D., Kossovich, L.Yu., Nolde, E.V., 1998. Dynamics of Thin Walled Elastic Bodies. Academic, San Diego.

Kaplunov, J., Kossovich, L., Zakharov, A., 2004. An explicit asymptotic model for the Blustein–Gulyaev wave. Comptes Rendus de Mécanique 332, 487–492.

Le, K.C., 1999. Vibrations of Shells and Rods. Springer Verlag, Berlin.

Lekhnitskii, S.G., 1968. Anisotropic Plates. Gordon and Breach, New York.

Li, Y., Thompson, R.B., 1990. Influence of anisotropy on the dispersion characteristics of guided ultrasonic plate modes. Journal of the Acoustical Society of America 87, 1911–1931.

Mindlin, R., 1951. Influence of rotary inertia and shear on flexural vibrations of isotropic, elastic plates. ASME Journal of Applied Mechanics 18, 31–38.

Muller, P., Touratier, M., 1995. On the so-called variational inconsistency of plate models, I. Indefinite plates: evaluation of the dispersive behaviour. Journal of Sound and Vibrations 188, 515–527.

Osborne, M.F.M., Hart, S.D., 1945. Transmission, reflection, and guiding of an exponential pulse by a steel plate in water. I. Theory. Journal of the Acoustical Society of America 17, 1–18.

Pham Chi Vinh, Ogden, R.W., 2004a. On formulas for the Rayleigh wave speed. Wave Motion 39, 191–197.

Pham Chi Vinh, Ogden, R.W., 2004b. Formulas for the Rayleigh wave speed in orthotropic elastic solids. Archives of Mechanics 56, 247–265.

Shuvalov, A.L., 2000. On the theory of wave propagation in anisotropic plates. Proceedings of the Royal Society London A 456, 2197–2222.

Shuvalov, A.L., 2002. Theory of subsonic elastic waves in fluid-loaded anisotropic plates. Proceedings of the Royal Society London A 458, 1323–1352.

Shuvalov, A.L., Poncelet, O., Baron, C., Deschamps, M., 2005. Long-wavelength dispersion of acoustic waves in transversely inhomogeneous anisotropic plates. Wave Motion 42, 367–382.

Solie, L.P., Auld, B.A., 1973. Elastic waves in free anisotropic plates. Journal of the Acoustical Society of America 54, 50–65.

Stephen, N.G., 1997. Mindlin plate theory: best shear coefficient and higher spectra validity. Journal of Sound and Vibrations 202, 539–553.

Ting, T.C.T., 1996. Anisotropic Elasticity. Oxford University Press, Oxford.